

**Spin-orbital fluctuations and a large mass enhancement in  $\text{LiV}_2\text{O}_4$** Yasufumi Yamashita<sup>1,2</sup> and Kazuo Ueda<sup>1,3</sup><sup>1</sup>*Institute for Solid State Physics, University of Tokyo, Kashiwa, Chiba 277-8581, Japan*<sup>2</sup>*Department of Physics, University of Cincinnati, Cincinnati, Ohio 45221*<sup>3</sup>*Advanced Science Research Center, Japan Atomic Energy Research Institute, Tokai, Ibaraki 319-1195, Japan*

(Received 2 December 2002; published 20 May 2003)

We present a scenario that the multicomponent fluctuations, especially those of the spin-orbital coupled modes, lead to the mass enhancement observed in  $\text{LiV}_2\text{O}_4$ . This phenomenon is possible because all these modes are fluctuating due to the geometrical frustration. To illustrate this mechanism, the  $t_{2g}$ -orbital Hubbard model on the pyrochlore lattice is studied based on the random-phase approximation. We derive the generalized susceptibility in the SU(6) spin-orbital space and calculate the free energy by using a coupling-constant integration. The estimated specific heat coefficient is of the correct order of magnitude to explain the experiment.

DOI: 10.1103/PhysRevB.67.195107

PACS number(s): 71.27.+a, 74.20.Mn, 71.28.+d

**I. INTRODUCTION**

The metallic spinel  $\text{LiV}_2\text{O}_4$  is a unique 3d heavy-fermion (HF) compound.<sup>1</sup> Its  $\gamma$  coefficient amounts to 420 mJ/mol K<sup>2</sup> and, strikingly, the low-temperature properties below  $T^* = 20 \sim 30$  are quite similar to those of the lanthanide or actinide HF compounds.<sup>1,2</sup> Since the  $d$  electrons, 1.5 per vanadium ion, are responsible for both transport and magnetism in  $\text{LiV}_2\text{O}_4$ , it is not trivial whether one can apply a scenario analogous to the conventional HF mechanism. Moreover, the large spatial extent of  $d$  orbitals compared with well-localized  $f$  orbitals is also unfavorable for the electrons to be treated as localized. In fact, some transport properties, such as the steep increase of resistivity above  $T^{*2}$  and the pressure-induced metal-insulator transition,<sup>3</sup> are different from those of the typical  $f$ -electron HF compounds.

Apart from the HF behavior, geometrical frustration is another specific feature of this system. The  $B$  site of the normal-spinel ( $\text{AB}_2\text{O}_4$ ) is known to form the network of corner-sharing tetrahedra (pyrochlore lattice). In most spinels, the geometric frustration is partially released by the structural phase transition. As a result, the ordered ground state is realized in the tetragonal phase, such as the possible charge ordering in  $\text{Fe}_3\text{O}_4$  or the Néel ordering in  $\text{ZnV}_2\text{O}_4$ .<sup>4</sup> In contrast,  $\text{LiV}_2\text{O}_4$  remains cubic and no static magnetic order was observed down to 0.02 K. The Curie-Weiss fit of the susceptibility ( $100 \leq T \leq 300$ ) results in an effective spin-1/2 moment per V with an antiferromagnetic (AF) coupling ( $\Theta_{\text{cw}} = -37$  K).<sup>2</sup> AF long-range order (LRO) will be suppressed by the geometric frustration and, indeed, the inelastic neutron scattering experiment captures the development of short-range AF correlations below  $|\Theta_{\text{cw}}|$ .<sup>5</sup> Interestingly enough, the large enhancement of  $\gamma$  is shared by other geometrically frustrated systems with strong AF spin fluctuations, such as  $\text{Y}(\text{Sc})\text{Mn}_2$  (Ref. 6) and  $\beta\text{-Mn}$ .<sup>7</sup> These facts seem to suggest that the formation of the heavy-mass  $d$  electron is related to the geometric frustration. In fact, the idea of connections between the heavy fermion behavior and magnetic frustration for pyrochlore lattice has been proposed in Ref. 8. In view of the geometric frustration, it should be

noted that, already at the 10% electron doping, the HF ground state is easily destroyed into the spin-glass phase.<sup>4</sup>

In  $\text{LiV}_2\text{O}_4$ , the crystal field around each V atom is nearly cubic with a slight trigonal distortion. The band-structure calculations indicate that the Fermi level lies within the cubic- $t_{2g}$  manifold with a bandwidth of about 2 eV,<sup>9-12</sup> which is actually the superposition of the two components, the relatively narrow  $A_{1g}$  ( $\sim 1$  eV) and the broad  $E_g$  orbital ( $\sim 2$  eV) of the  $D_{3d}$  group. Matsuno, Fujimori, and Mattheiss considered this trigonal split less important, and stressed the importance of the geometric frustration and/or orbital degeneracy.<sup>10</sup> On the other hand, the LDA+ $U$  calculation by Anisimov *et al.* suggested that the correlation effect leads to the orbital polarization, where the  $A_{1g}$  orbital is occupied singly to form a localized spin-1/2 moment and the rest 0.5 electron fills the  $E_g$  band. Thereby, they proposed the Kondo scenario based on the effective Anderson impurity model.<sup>9</sup>

Followed by these band-structure calculations, various theoretical models are proposed in connection with the microscopic origin of the 3d HF behavior.<sup>13-19</sup> Especially, the role of the geometric frustration has been featured in recent studies. Motivated by the Curie-Weiss law around room temperature, the formation of the localized  $s = 1/2$  is assumed by several authors on the grounds of the orbital polarization<sup>16,17</sup> or the local valence fluctuations.<sup>18</sup> In these treatments the spin frustration is their main concern.<sup>19</sup>

In this paper, we consider that the present system realizes the prototypical itinerant frustrated model and a realistic model Hamiltonian of the  $t_{2g}$ -band pyrochlore Hubbard model is investigated with particular emphasis on orbital fluctuations. Within the random-phase approximation (RPA) scheme, all kinds of fluctuations are included simultaneously without prejudice. In principle, geometric frustration prevents any kinds of LRO and thus the large  $\gamma$  would be expected by the resultant enhanced fluctuations. In this scenario, not only the spin but also both of the orbital and spin-orbital fluctuations are responsible for the enhancement. To our knowledge, this is the first theoretical attempt to attribute the heavy-mass  $d$  electron directly to the orbital degrees of freedom. The instability itself of the same model was dis-

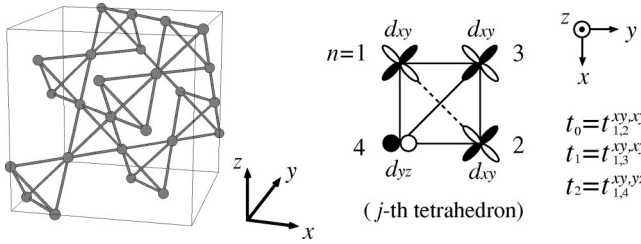


FIG. 1. The cubic unit cell of the pyrochlore lattice (left panel) and the three independent hoppings (right).

discussed by Tsunetsugu.<sup>20</sup> We have explicitly calculated the  $T$ -linear coefficient of the imaginary part of the generalized susceptibility and found the large enhancement of  $\gamma$  mainly due to the spin-orbital fluctuations.

## II. MODEL HAMILTONIAN

The pyrochlore lattice is a fcc array of tetrahedra. The cubic unit cell shown in Fig. 1 contains 16 lattice points covered by four tetrahedra and the primitive unit cell includes a single tetrahedron. Therefore the  $t_{2g}$  electrons are specified by the following four indices; the unit cell (denoted by  $j=1, \dots, 4L^3$ ), the sublattice ( $n=1, \dots, 4$ ), the orbital ( $m=d_{xy}, d_{yz}, d_{zx}$ ), and the spin ( $\sigma=\uparrow/\downarrow$ ), where  $L$  is the number of the cubic unit cell along one direction. By using the standard notation of the multiband Hubbard model, the  $t_{2g}$ -band Hubbard model on the pyrochlore lattice is given by  $\mathcal{H}=\mathcal{H}_0+\mathcal{H}_1$ ,

$$\mathcal{H}_0 = \sum_{k\sigma mm'n'} t_{nn'k}^{mm'} c_{kmm\sigma}^\dagger c_{km'n'\sigma}, \quad (1)$$

$$\mathcal{H}_1 = \sum_{jn} \left\{ U \sum_m n_{jmn\uparrow} n_{jmn\downarrow} + U' \sum_{m>m'\sigma\sigma'} n_{jmn\sigma} n_{jm'n\sigma'} - J \sum_{m>m'\sigma\sigma'} c_{jmn\sigma}^\dagger c_{jmn\sigma'} c_{jm'n\sigma'}^\dagger c_{jm'n\sigma} \right\}. \quad (2)$$

Here  $t_{nn'}^{mm'}$  is the transfer integral between the  $m$  orbital at  $n$  sublattice and the  $m'$  orbital at  $n'$  sublattice when  $(m,n) \neq (m',n')$ . In addition, the parameter of  $t_{nn'}^{mm'} (= \pm D/3)$  type is also included to describe the trigonal split of  $t_{2g}$ ,  $E_{a_{1g}} - E_{e_g} = D$ . Since the nearest-neighbor (NN) hoppings already depend on the bond direction and the orbital symmetry, the NN tight-binding model would be sufficient for the present study. By the symmetry relation, all the hopping matrices are represented by the following three independent parameters:  $t_0 = t_{12}^{xy,xy}$ ,  $t_1 = t_{13}^{xy,xy}$ , and  $t_2 = t_{14}^{xy,yz}$ . The  $T_d$  symmetry of the unit cell as well as the spin SU(2) are incorporated in the  $12 \times 12$  matrix  $\mathcal{H}_0$ , though here we do not display the matrix explicitly.

The tight-binding fit of the linear augmented-plane-wave band-structure calculation gives the parameters in  $\mathcal{H}_0$  to be  $t_0 = -0.281$  eV,  $t_1 = -t_2 = 0.076$  eV, and  $D = 0.140$  eV.<sup>10</sup> By applying the orthogonal transformation  $c_{k\mu\sigma} = \sum_\nu U_{\mu\nu}(k) a_{k\nu\sigma}$ , the single-electron Hamiltonian is diago-

nized into  $\mathcal{H}_0 = \sum_{k\sigma\nu} \epsilon_{k\nu} a_{k\nu\sigma}^\dagger a_{k\nu\sigma}$ , where  $\mu=(m,n)$  and  $\nu$  are 12-dimensional indices. The calculated  $t_{2g}$ -multiplet ( $\epsilon_{k\nu}, \nu=1, \dots, 12$ ) are shown in Fig. 2 along some typical symmetric lines. The almost flat bands near the Fermi level results in high density of state (DOS) at the Fermi level. Actually, the  $\gamma$  coefficient estimated from the DOS of the band-structure calculation is relatively large;  $\gamma_{\text{band}} \sim 17$  mJ/mol K.<sup>10</sup> However, the experimentally observed value ( $\gamma_{\text{exp}}$ ) is about 25 times larger than  $\gamma_{\text{band}}$ . As a possible origin of this enhancement, in the following, we consider the effect of electron correlations from the weak-coupling limit.

Finally, we comment on the difference between the present band structure and that in Ref. 20. In Ref. 20, the completely degenerate  $t_{2g}$  orbitals are considered, that is,  $D=0$ , and the hopping parameters are also different from ours.

## III. FREE ENERGY AND RPA EQUATIONS

In order to describe various kinds of fluctuations concerning the  $t_{2g}$  electrons in a simple way, we introduce 35 generators of the SU(6) group  $X^\gamma (\gamma=1, \dots, 35)$  and the identity operator  $X^0$ , where the normalization condition is  $\text{Tr} X^\gamma X^{\gamma'} = \delta^{\gamma\gamma'}/2$ . The SU(6) generators are classified into the pure spin, the pure orbital, and the spin-orbital coupled components. Spin and orbital degrees of freedom are described by the generators of SU(2) ( $S^\alpha$ ; three dimensions) and SU(3) ( $T^\beta$ ; eight dimensions) groups, respectively, and the spin-orbital coupled modes are made of the products of the two ( $2\sqrt{3}S^\alpha T^\beta$ ; 24 dimensions). To be explicit, these operators are represented by using the electron creation and annihilation operators as follows:

$$X_{jn}^0 = \frac{1}{2\sqrt{3}} \sum_{\sigma m} c_{jmn\sigma}^\dagger c_{jmn\sigma}, \quad (3)$$

$$S_{jn}^\alpha = \frac{1}{2\sqrt{3}} \sum_{\sigma\sigma'm} c_{jmn\sigma}^\dagger \sigma_{\sigma\sigma'}^\alpha c_{jmn\sigma'}, \quad (4)$$

$$T_{jn}^\beta = \frac{1}{2\sqrt{2}} \sum_{\sigma mm'} c_{jmn\sigma}^\dagger \lambda_{mm'}^\beta c_{jmn\sigma}, \quad (5)$$

$$2\sqrt{3}S^\alpha T_{jn}^\beta = \frac{1}{2\sqrt{2}} \sum_{\sigma\sigma'mm'} c_{jmn\sigma}^\dagger \sigma_{\sigma\sigma'}^\alpha \lambda_{mm'}^\beta c_{jmn\sigma'}, \quad (6)$$

where  $\vec{\sigma}$  and  $\vec{\lambda}$  are the Pauli and the Gell-Mann matrices in the standard notations,<sup>21</sup> respectively. Note that the overall signs of nondiagonal operators for different sublattices are selected to be consistent with the  $T_d$  unit-cell symmetry. Since the trigonal distortion in  $\mathcal{H}_0$  violates the  $O(3)$  orbital symmetry, the usual representations of the  $t_{2g}$  orbital by the fictitious  $\vec{l}=1$  and its higher moments do not reflect the proper symmetry. Instead we construct the tensor products of the real  $\vec{l}=2$  moment and reduce them into the irreducible representations of  $T_d$  in the cubic  $t_{2g}$  subspace. As a result,

TABLE I. The matrix elements of the diagonal interaction matrices,  $\Lambda_{\beta\beta'}^{(c/s)}$ , for each irreducible representation.

	$A_1(\beta=0)$	$\Gamma_5(1,4,6)$	$\Gamma_5(2,5,7)$	$\Gamma_3(3,8)$
$\Lambda_{\beta\beta}^{(c)}$	$-U-4U'+2J$	$U'-2J$	$U'-2J$	$-U+2U'-J$
$\Lambda_{\beta\beta}^{(s)}$	$U+2J$	$U'$	$U'$	$U-J$

we find that  $\vec{\lambda}$  is the proper set of basis, which is classified into three irreducible representations;  $\Gamma_5$ -dipolar moments ( $\lambda_2, \lambda_5, \lambda_7$ ),  $\Gamma_5$ -quadrupolar moments ( $\lambda_1, \lambda_4, \lambda_6$ ), and  $\Gamma_3$ -quadrupolar moments ( $\lambda_3, \lambda_8$ ).

Next we transform the interaction part of the Hamiltonian in terms of  $X^\gamma$ 's so that

$$\mathcal{H}_I = \sum_{jn} \sum_{\gamma=0}^{35} a_{\gamma\gamma} X_{jn}^\gamma X_{jn}^\gamma, \quad (7)$$

except for a constant energy shift. Here  $a_{\gamma\gamma}$ 's are functions of  $U, U'$ , and  $J$ . Such transformation is always possible for any  $U, U'$ , and  $J$ , though the choice of  $a_{\gamma\gamma}$  is not unique because of the spin-rotational invariance and/or the identity  $n_{jmn\sigma}^2 = n_{jmn\sigma}$ . By applying a coupling constant integration together with Eq. (7), the free energy for this system is given by

$$F(U, U', J) = F(0) + \frac{1}{2\pi} \int_{-\infty}^{\infty} d\omega \coth\left(\frac{\beta\omega}{2}\right) \times \sum_{qn} \sum_{\gamma} a_{\gamma\gamma} \int_0^1 dx \text{Im} \chi_{nn}^{\gamma\gamma}(q, \omega)|_{xU, xU', xJ}, \quad (8)$$

where the momentum sum is taken all over the first Brillouin zone, and the generalized susceptibility per tetrahedron is defined by

$$\chi_{nn'}^{\gamma\gamma'}(\vec{q}, \omega) = \frac{i}{4L^3} \int_0^\infty d\tau e^{i(\omega+i\delta)\tau} \langle [X_{qn}^\gamma(\tau), X_{-qn'}^{\gamma'}(0)] \rangle. \quad (9)$$

We apply the RPA in the evaluation of the generalized susceptibility ( $\chi$ ). Including the charge degree of freedom ( $X^0$ ), our  $\chi$  is the  $144 \times 144$  matrix with the row index  $n\gamma$  and the column  $n'\gamma'$ . Since we are concerned with the paramagnetic state, as suggested by the experiment, the  $SU(2)$  symmetry ensures that  $\chi$  is decomposed into the spin singlet and triplet sectors. Each sector is represented by the charge-charge (denoted by  $\chi_{nn'}^{\beta\beta'(c)}$ ) and the  $S^z$ - $S^z$  susceptibilities ( $\chi_{nn'}^{\beta\beta'(s)}$ ), respectively. In these two  $36 \times 36$  matrices, the spin index ( $\alpha$ ) is reduced and the remaining indices are the row index  $n\beta$  and the column index  $n'\beta'$ . Here  $\beta=0$  is defined to represent the totally symmetric orbital operator. To sum up,  $\chi_{nn'}^{\beta\beta'(c)}$  describes the correlations among the charge ( $\beta=0$ ) and the orbital ( $\beta \geq 1$ ), while  $\chi_{nn'}^{\beta\beta'(s)}$  among the spin ( $\beta=0$ ) and the spin orbital ( $\beta \geq 1$ ). By using these notations, the RPA equations are given as follows:

$$\chi_{nn'}^{\beta\beta'(c/s)} = \chi_{nn'}^{\beta\beta'(0)} + \sum_{n_1\beta_1} \chi_{nn_1}^{\beta\beta_1(0)} 2\Lambda_{\beta_1\beta_1}^{(c/s)} \chi_{n_1n'}^{\beta_1\beta'(c/s)}, \quad (10)$$

Since the interaction is local, the interaction matrices ( $\Lambda^{(c/s)}$ ) are always  $n$ -diagonal and independent of  $n$ . Thus, the remaining indices are row  $\beta$  and column  $\beta'$ . Moreover, the  $9 \times 9$  matrices  $\Lambda^{(c/s)}$  may have a simple representation. This is because  $\mathcal{H}_0$  has the  $T_d$  symmetry and Eq. (10) is invariant under any  $T_d$  transformation. Therefore,  $\Lambda^{(c/s)}$ 's must be diagonal and these matrix elements are the same within each irreducible representation, see Table I.

$\chi_{nn'}^{\beta\beta'(0)}$  in Eq. (10) is the paramagnetic susceptibility of the Hartree-Fock approximation. When we calculate  $\chi^{(0)}$  of the usual single band Hubbard model, the Hartree-Fock terms just renormalize the chemical potential. In our model the Hartree term similarly changes the diagonal part of  $\mathcal{H}_0$ , whereas the Fock terms introduce off-diagonal terms of the orbital hoppings on the same site, giving rise to the crystal field effect. This crystal field is totally symmetric concerning the entire unit cell, but its local symmetry on each sublattice is trigonal. The effect of this additional field is included in the band-structure calculations. Therefore, the free paramagnetic susceptibility calculated by using the tight-binding parameters gives the appropriate  $\chi_{nn'}^{\beta\beta'(0)}$ . In the actual calculation, we used the free  $\chi^{(0)}$  per tetrahedron of the form

$$\chi_{\mu_1\mu_2\mu_3\mu_4}^{(0)}(q, \omega) = \frac{1}{4L^3} \sum_k \sum_{\nu_1\nu_2} \frac{f(\epsilon_{k+q\nu_2}) - f(\epsilon_{k\nu_1})}{\epsilon_{k\nu_1} - \epsilon_{k+q\nu_2} + \hbar(\omega + i\delta)} \times U_{\mu_1\nu_1}(k) U_{\mu_4\nu_1}(k) U_{\mu_2\nu_2}(k+q) \times U_{\mu_3\nu_2}(k+q), \quad (11)$$

and rotated the orbital basis from  $\{m_1 m_2 m_3 m_4\}$  into  $\{\beta\beta'\}$ , where  $f(\epsilon)$  is the Fermi distribution function.

#### IV. ESTIMATION OF THE SPECIFIC HEAT COEFFICIENT

Since we are primarily interested in the mass enhancement in  $\gamma$ , let us now focus on the  $\omega$ -linear part of  $\text{Im} \chi$  in the free energy of Eq. (8). As seen from the band structure (Fig. 2), nothing singular would happen in  $\chi^{(0)}$ ; therefore a constant  $\text{Re} \chi^{(0)}$  and an  $\omega$ -linear  $\text{Im} \chi^{(0)}$  behaviors are expected in the leading order of  $\omega$ . Then it is sufficient to solve the RPA equations in the lowest order of  $\text{Im} \chi^{(0)} \propto \omega$ . For the half-filled  $s$ -band pyrochlore Hubbard model, in contrast, the complete matching of the Fermi level and flat bands brings a non-Fermi liquid behavior.<sup>22,23</sup> As for the still-unfixed  $a_{\gamma\gamma}$ , we take

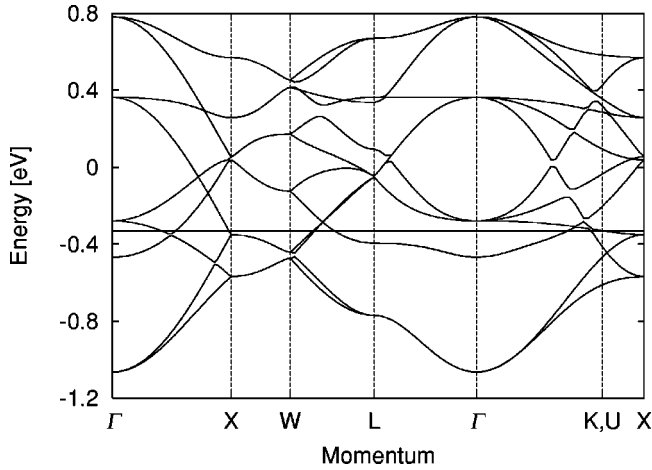


FIG. 2. Band structure of the  $t_{2g}$  multiplet for the present parameter along symmetric lines of the fcc Brillouin zone. The horizontal straight line is the Fermi level for the quarter filling.

$$a_{\gamma\gamma} = -\frac{1}{2}\Lambda_{\gamma\gamma} = -\frac{1}{2}(\Lambda^{(c)} \oplus \Lambda^{(s)} \oplus \Lambda^{(s)} \oplus \Lambda^{(s)}). \quad (12)$$

It is easy to check that the  $a_{\gamma\gamma}$ 's of this form reproduce the original interaction term, Eq. (7). This choice is natural in the sense that  $\Lambda_{\gamma\gamma}$  reflects the symmetry of the noninteraction term  $[\text{SU}(2)$  and  $T_d]$ . We neglect the weak dependence of  $\chi^{(0)}$  on the interaction through the Fock terms for simplicity, then the  $x$  integral in Eq. (8) can be performed analytically. After some calculations,  $\gamma$  coefficient ( $= -\partial^2 F / \partial^2 T$ ) per tetrahedron is given by

$$\gamma_{\text{RPA}} = \sum_{\beta=0}^8 (\gamma^{\beta(c)} + 3\gamma^{\beta(s)}), \quad (13)$$

with

$$\begin{aligned} \gamma^{\beta(c/s)} = & \frac{\pi k_B^2}{12L^3} \sum_{qn} \sum_{n_1\beta_1} \Lambda_{\beta\beta}^{(c/s)} \frac{\text{Im}\chi_{nn_1}^{\beta\beta_1(0)}(\vec{q}, \omega)}{\omega} \\ & \times (1 - 2\Lambda_{\beta_1\beta_1}^{(c/s)} \text{Re}\chi_{n_1n}^{\beta_1\beta_1(0)}(\vec{q}, \omega))^{-1}. \end{aligned} \quad (14)$$

This equation is exact after taking  $\omega, \delta, T \rightarrow 0$  and  $L \rightarrow \infty$  limit. Note that we neglect the zero-point fluctuation term in the  $\omega$  integral because it will only show a weak temperature dependence through that of  $\chi^{(0)}$ .

Finally we numerically estimate  $\gamma_{\text{RPA}}$  in the  $\text{SU}(6)$  limit ( $U = U'$  and  $J = 0$ ), where the orbital fluctuations are mostly enhanced. For this purpose, we calculated the free susceptibility, Eq. (11), for the parameter set of  $(\omega, \delta, T) = (0.02 \text{ eV}, 0.02 \text{ eV}, 0.02 \text{ eV})$  and  $L = 16$ . We checked the convergence of  $\chi^{(0)}$  against  $\omega$  and  $L$  along some symmetric lines. Especially, we confirmed that  $\text{Im}\chi^{(0)}$  shows a clear  $\omega$ -linear dependence in the range of  $\omega = 0.01, 0.02, 0.04, 0.08 \text{ eV}$ . The convergence of the  $\omega$ -linear coefficient regarding the system size ( $L = 12, 16, 24, 32$ ) is fairly good except for a few points very close to the  $\Gamma$  point. As a result, we obtained the  $\gamma$  value per  $\text{LiV}_2\text{O}_4$  mole, as shown in Fig. 3. The total  $\gamma$  is the summation of the contributions from charge (denoted by  $\gamma_c = \gamma^{0(c)}$ ), spin ( $\gamma_s$

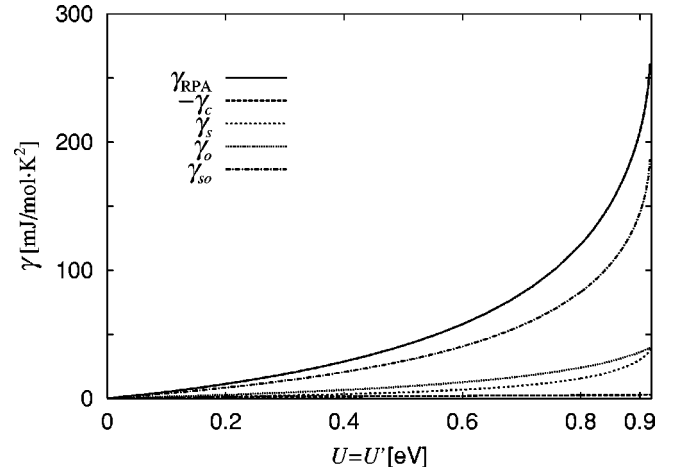


FIG. 3. The graph shows  $\gamma$  value per formula unit of  $\text{LiV}_2\text{O}_4$  mole. The contributions from charge, spin, orbital, and spin-orbital fluctuations are labeled by  $\gamma_c$ ,  $\gamma_s$ ,  $\gamma_o$ , and  $\gamma_{so}$ , respectively.

$= 3\gamma^{0(s)}$ ), orbital ( $\gamma_o = \sum_{\beta=1}^8 \gamma^{\beta(c)}$ ), and spin-orbital fluctuations ( $\gamma_{so} = 3\sum_{\beta=1}^8 \gamma^{\beta(s)}$ ). The critical value  $U_c$  is about 0.92 eV and there the complicated eigenvectors, made of the four sublattice summations of the spin and spin-orbital components with quadrupole orbital modes, characterize the instability at the wave vector near  $\Gamma$  point. Since we fixed  $\omega$  finite and took the limit  $\vec{q} \rightarrow 0$ , our calculated  $\text{Re}\chi^{(0)}$  does not correspond to the  $\omega \rightarrow 0$  limit at  $\Gamma$  point. Therefore we cannot determine that the most prominent modes are just at the  $\Gamma$  point or not. The real part of  $\chi^{(0)}$  is studied for different hopping parameters at zero temperature.<sup>20</sup> In the present calculation, we do not detect the peak structure around  $X$  and  $L_2$  points found in Ref. 20. The reason for the difference might be that our calculations have done at finite  $T$  and/or these single modes are quite sensitive to the nesting of the Fermi surface.

Figure 3 shows that the correct order of  $\gamma$  can be reproduced even away from the critical point, say  $\sim 0.8U_c$ . Around there, the enhancement of  $\gamma_{\text{RPA}}$  (about 80%) is mainly attributed to the various spin-orbital fluctuations. Both spin and spin-orbital fluctuations contribute  $\gamma_{\text{RPA}}$  by the same order as a single component. However, the magnitude of the components, 3 for spin and 24 for spin-orbital modes, results in the different contribution in  $\gamma_{\text{RPA}}$ . In order to gain the same enhancement solely by the spin fluctuations,  $U$  must be very close to  $U_c$  eVen after the inclusion of  $J$  term. Away from  $U_c$ , the enhancement of  $\gamma_{\text{RPA}}$  comes from the entire momentum space because the spin and spin-orbital fluctuations have rather weak  $q$  dependences. This result seems to be consistent with the naive picture that the geometric frustration induces local fluctuations, which is responsible for the heavy mass.

## V. CONCLUSION

In conclusion we have studied the origin of the large enhancement of  $\gamma$  in  $\text{LiV}_2\text{O}_4$  based on the one-fourth-filled  $t_{2g}$ -band pyrochlore Hubbard model. We introduced  $T_d$  irreducible operators for orbital density operators and derived

the RPA equations in a simple form. The  $\gamma_{\text{RPA}}$  obtained by the coupling constant integration of  $\text{Im}\chi$  is enhanced typically by the order of 10 due to the spin-orbital fluctuations compared with the  $\gamma_s$  due to the spin alone. This conclusion itself seems to be general for the orbital disordered system, and thus it may be possible to apply the present scenario to other systems, such as  $\text{Y}(\text{Sc})\text{Mn}_2$  and  $\beta\text{-Mn}$ . To be more specific to  $\text{LiV}_2\text{O}_4$ , the calculated  $\gamma_{\text{RPA}}$  value is of the same order as  $\gamma_{\text{exp}}$ . However, it should be noted that our simple theory does not include the effect of the geometrical frustrations sufficiently, since the mode-mode coupling between various fluctuations is neglected. In general, the RPA approximation overestimates the fluctuations; therefore the most prominent mode itself would be suppressed and  $U_c$  becomes larger if we include the couplings between the modes with different momenta. At the same time, the overall structure of  $\chi$  in  $q$  space would change into more and more structureless and thus the additional enhancement of  $\gamma$  could be expected.

It is well known that the mode-mode coupling theory leads to the Curie-Weiss behavior of the magnetic susceptibility. As for the  $R_W$ , it is of the order of 0.1 in the RPA approximation. This value would be increased by including  $J$ , although it is not clear whether the Hund's rule coupling is sufficient to obtain  $R_W \sim 1.7$ . To address the similarity to the  $4f$  HF compounds, we need to develop a more sophisticated theory including the coupling between fluctuations. The fluctuation exchange approximation for the multiband model would be useful as the next step.

#### ACKNOWLEDGMENTS

We thank H. Tsunetsugu for sending us his related work<sup>20</sup> prior to the publication. Y.Y. is supported by the Japan Society for the Promotion of Science (JSPS). K.U. is supported by Grant-in-Aid for Scientific Research from the JSPS.

- 
- <sup>1</sup>S. Kondo *et al.*, Phys. Rev. Lett. **78**, 3729 (1997).  
<sup>2</sup>C. Urano, M. Nohara, S. Kondo, F. Sakai, H. Takagi, T. Shiraki, and T. Okubo, Phys. Rev. Lett. **85**, 1052 (2000).  
<sup>3</sup>C. Urano (private communication).  
<sup>4</sup>Y. Ueda, N. Fujiwara, and H. Yasuoka, J. Phys. Soc. Jpn. **66**, 778 (1997).  
<sup>5</sup>S.-H. Lee, Y. Qiu, C. Broholm, Y. Ueda, and J.J. Rush, Phys. Rev. Lett. **86**, 5554 (2001).  
<sup>6</sup>M. Shiga, K. Fujisawa, and H. Wada, J. Phys. Soc. Jpn. **62**, 1329 (1993).  
<sup>7</sup>H. Nakamura, K. Yoshimoto, M. Shiga, M. Nishi, and K. Kakurai, J. Phys.: Condens. Matter **9**, 4701 (1997).  
<sup>8</sup>V.Yu. Irkhin and M.I. Katsnelson, Phys. Lett. A **150**, 47 (1990).  
<sup>9</sup>V.I. Anisimov, M.A. Korotin, M. Zöhl, T. Pruschke, K. Le Hur, and T.M. Rice, Phys. Rev. Lett. **83**, 364 (1999).  
<sup>10</sup>J. Matsuno, A. Fujimori, and L.F. Mattheiss, Phys. Rev. B **60**, 1607 (1999).  
<sup>11</sup>V. Eyert, K.-H. Höck, S. Horn, A. Loidl, and P.S. Riseborough, Europhys. Lett. **46**, 762 (1999).  
<sup>12</sup>D.J. Singh, P. Blaha, K. Schwarz, and I.I. Mazin, Phys. Rev. B **60**, 16 359 (1999).  
<sup>13</sup>H. Kusunose, S. Yotsuhashi, and K. Miyake, Phys. Rev. B **62**, 4403 (2000).  
<sup>14</sup>P. Flude, A.N. Yaresko, A.A. Zvyagin, and Y. Grin, Europhys. Lett. **54**, 779 (2001).  
<sup>15</sup>S. Fujimoto, Phys. Rev. B **65**, 155108 (2002).  
<sup>16</sup>C. Lacroix, Can. J. Phys. **70**, 1469 (2002).  
<sup>17</sup>M. Laad, L. Craco, and E. Muller-Hartmann, cond-mat/0202531 (unpublished).  
<sup>18</sup>J. Hopkinson and P. Coleman, cond-mat/0203288 (unpublished).  
<sup>19</sup>S. Burdin, D.R. Grempel, and A. Georges, Phys. Rev. B **66**, 045111 (2002).  
<sup>20</sup>H. Tsunetsugu, J. Phys. Soc. Jpn. **71**, 1844 (2002).  
<sup>21</sup>X. Hamermesh, *Group Theory* (Addison-Wesley, Reading, Massachusetts, 1962).  
<sup>22</sup>M. Isoda and S. Mori, J. Phys. Soc. Jpn. **69**, 1509 (2000).  
<sup>23</sup>S. Fujimoto, Phys. Rev. B **64**, 085102 (2001).